Accepted Manuscript

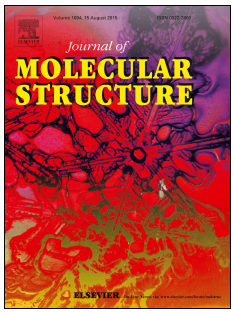

Structural and spectroscopic investigation on a new potentially bioactive di-hydrazone containing thiophene heterocyclic rings

Vanessa de S. Nogueira, Maria Clara Ramalho Freitas, Wellington S. Cruz, Tatiana S. Ribeiro, Jackson A.L.C. Resende, Nicolás A. Rey

PII: S0022-2860(15)30381-1

DOI: 10.1016/j.molstruc.2015.10.081

Reference: MOLSTR 21926

To appear in: *Journal of Molecular Structure*

Received Date: 22 July 2015

Revised Date: 21 October 2015

Accepted Date: 26 October 2015

Please cite this article as: V.d.S. Nogueira, M.C. Ramalho Freitas, W.S. Cruz, T.S. Ribeiro, J.A.L.C. Resende, N.A. Rey, Structural and spectroscopic investigation on a new potentially bioactive di-hydrazone containing thiophene heterocyclic rings, *Journal of Molecular Structure* (2015), doi: 10.1016/j.molstruc.2015.10.081.

Graphical abstract

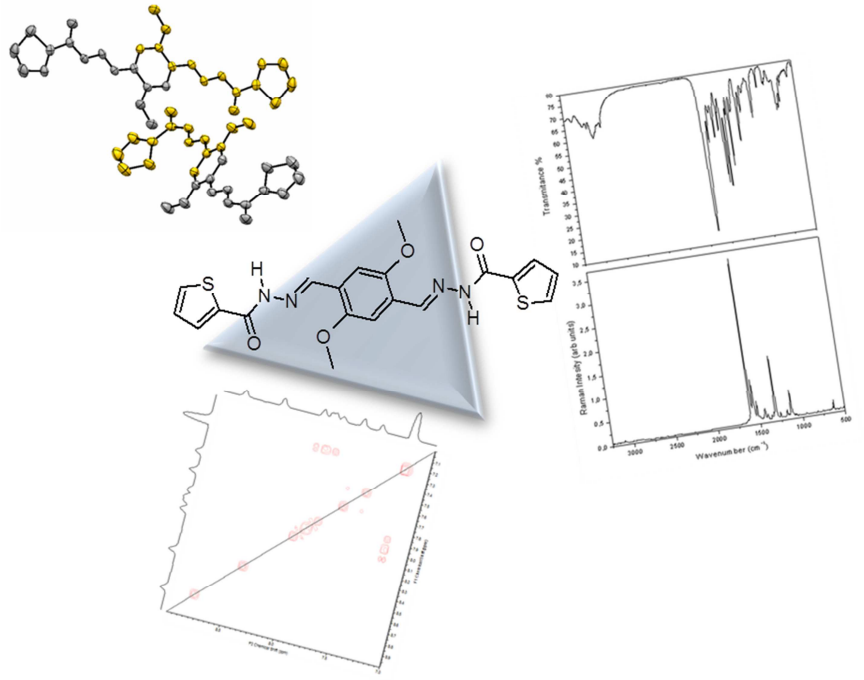

Structural and spectroscopic investigation on a new potentially bioactive di-hydrazone containing thiophene heterocyclic rings

Vanessa de S. Nogueira[a], Maria Clara Ramalho Freitas[b], Wellington S. Cruz[a], Tatiana S. Ribeiro[c], Jackson A. L. C. Resende[b], Nicolás A. Rey[a,*]

**nicoarey@puc-rio.br*

[a] *Department of Chemistry, PUC-Rio, Rua Marquês de São Vicente, 225 – 22453-900, Rio de Janeiro, RJ, Brazil*

[b] *Institute of Chemistry, UFF, Outeiro de São João Batista, s/n – 24020-141, Niterói, RJ, Brazil*

[c] *DCNME, UFSCar, Rodovia Anhanguera, km 174– 13600-970, Araras, SP, Brazil*

Abstract

Hydrazones and several substituted hydrazones are associated with a broad spectrum of biological activities, as well as compounds containing the thiophene ring. In this context, a novel di-hydrazone derived from 2-thiophenecarboxylic acid hydrazide was synthesized and completely characterized by elemental analysis, XRD, FT-IR, Raman and UV-Vis spectroscopies, thermogravimetry, ^{1}H NMR, ^{1}H-^{1}H COSY and ^{1}H-^{1}H ROESY. A preliminary *in silico* pharmacological evaluation was also performed in order to assess the performance of the new compound regarding some molecular properties relevant for a drug's pharmacokinetics in the human body.

Keywords: Di-hydrazone; Thiophene; Synthesis; X-ray diffraction; Spectroscopy

1. Introduction

Hydrazones are a class of organic compounds defined by the presence of the functional group $R_1R_2C{=}N{-}NR_3R_4$ [1]. Literature studies reveal that hydrazones and several substituted hydrazones are associated with a broad spectrum of biological activities, such as analgesic [2], antihypertensive [3], anticonvulsant [4], anti-inflammatory [5], anti-TB [6, 7], antitumor [8, 9], anti-HIV [10, 11], antimalarial [12], antidepressant [13], and vasodilatory [14]. Very recently, anti-Alzheimer activity was also reported for hydrazones derived from 8-hydroxyquinoline-2-carboxaldehyde [15, 16]. It is known that the interesting biological properties of carbonyl-containing hydrazones are related to the presence of the $R_1R_2C{=}N{-}NH{-}CO{-}$ pharmacophore [1], which also allows for those compounds to act as bidentate ligands, coordinating biometals through the azomethine nitrogen and the carbonyl

oxygen. Our research group at the Pontifical Catholic University of Rio de Janeiro (PUC-Rio) has some experience in the synthesis of heterocyclic hydrazones [17, 18].

On the other hand, thiophene belongs to a class of heterocyclic sulfur compounds containing a five-membered ring [19]. Its structure is similar to that of pyrrole and constitutes one of the most important classes of heterocycles, presenting a variety of actions [20], such as antimicrobial [21, 22], antitumoral [23], analgesic and anti-inflammatory [24], antihypertensive [25], anti-diabetes [26], inhibitory activity of cholesterol [27], anti-allergic [28], insecticide [29] and antioxidant [30]. Thiophene can be attached to various heterocyclic systems giving rise to new compounds, which exhibit a broad range of biological effects, and reduced toxicity [31].

In view of the intrinsic biological relevance of both hydrazones and tiophene, and based on the well-known concept of hybrid drugs, this paper reports on the synthesis of a novel di-hydrazone, obtained by condensation between 2,5-dimethoxyterephthalaldehyde and 2-thiophenecarboxylic acid hidrazide. This compound was characterized by elemental analysis, X-ray crystallography, FT-IR, Raman and UV-Vis spectroscopies, thermogravimetry, ^{1}H NMR, ^{1}H-^{1}H COSY and ^{1}H-^{1}H ROESY experiments. A preliminary *in silico* (computational) pharmacological evaluation was also performed in order to assess the performance of the synthesized compound regarding some molecular properties relevant for a drug's pharmacokinetics in the human body.

2. Experimental methods

2.1. Syntheses of the target compound and its precursors

For the preparation of the desired di-hydrazone, we chose a protocol that involves the synthesis of a symmetrical precursor center, namely, 2,5-dimethoxyterephthalaldehyde, which is obtained from 2,5-bis(chloromethyl)-1,4-dimethoxybenzene. This compound was, in turn, prepared from the starting material 1,4-dimethoxybenzene (**Scheme 1**, top). All chemicals were purchased from commercial sources and used without further purification.

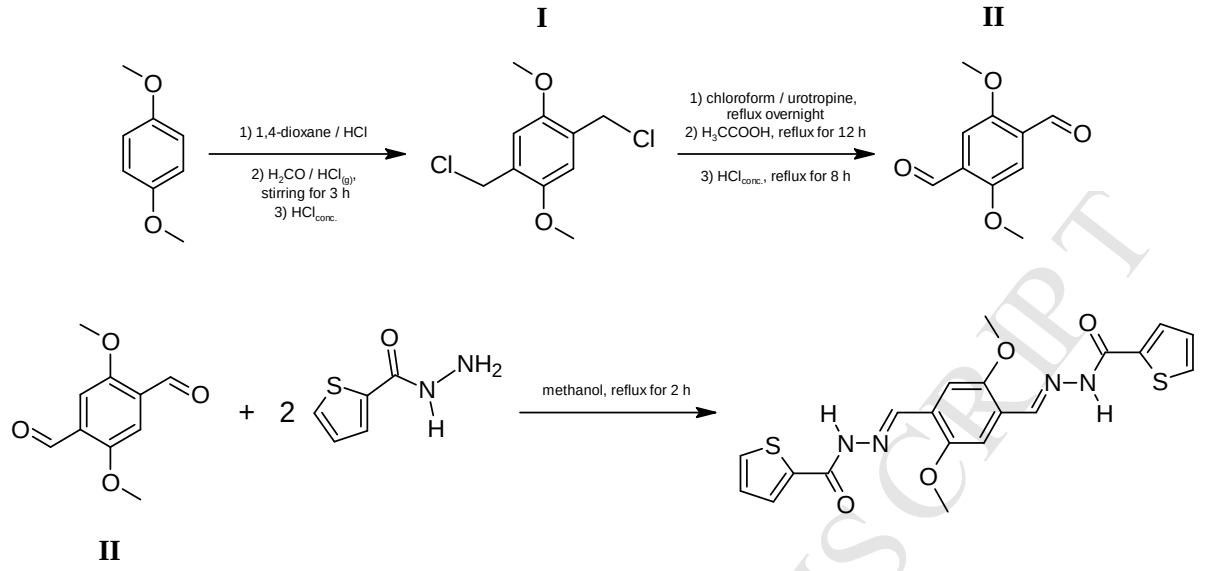

Scheme 1. Chemical synthesis of 2,5-dimethoxyterephthalaldehyde bis(thiophene-2-carbonyl hydrazone).

2.1.1. 2,5-bis(chloromethyl)-1,4-dimethoxybenzene (I)

This compound was prepared in the way described in literature [32]. Yield: 39.3g (23%) of a white powder, m.p. 164 ºC (literature m.p.: 165 ºC). **Main IR bands** (KBr): 3050, 3019, 2966, 2938, 2837, 1512, 1464, 1432, 1409, 1319, 1259, 1224, 1179, 1136, 1041, 913, 877, 736, 680, 609, 475 cm^{-1}. **^{1}H NMR** (DMSO-d_6, 300 MHz): 3,78 ppm (s, 6H, –OCH_3); 4,67 ppm (s, 4H, –CH_2Cl); 7,12 ppm (s, 2H, aromatic ring).

2.1.2. 2,5-dimethoxyterephthalaldehyde (II)

This precursor center was prepared in three synthetic steps, from a procedure involving small modifications of the method already reported [33]. Initially, we dissolved 24.1 g (0.10 mol) of **I** and 30.0 g (0.21 mol) of urotropine (hexamethylenetetramine) in 200 mL of chloroform. The mixture was refluxed overnight. At the end of this first stage, after leaving the mixture cool to room temperature, the solvent was removed under reduced pressure and the solid residue obtained was dissolved in 320 mL of a 50% acetic acid aqueous solution, being refluxed subsequently for 12 hours. In the last part of the process, 25 mL of concentrated HCl was dropwise added to the solution, which was then refluxed for 8 hours. After cooling, we observed the formation of a yellow precipitate, which was filtered off, washed with cold water and ethanol and dried under vacuum. Yield: 2.1 g (~10%), m.p. 207 ºC (literature m.p.: 207 ºC). From the filtrate, an additional 0.8 g of the product could be obtained; its m.p. was 200 ºC. The substance was used in the next step without

further purification. Elemental analysis - Percentages found: C, 61.9; H, 5.2. Calcd. for $C_{10}H_{10}O_4$: C, 61.9;H, 5.2. **Main IR bands** (KBr): 3435, 3069, 3048, 2992, 2953, 2932, 2870, 2833, 1679, 1503, 1483, 1466, 1408, 1398, 1302, 1131, 1042, 878, 660 cm^{-1}. **^{1}H NMR** ($CDCl_3$, 300 MHz): 3,93 ppm (s, 6H, –OC*H*$_3$); 7,44 ppm (s, 2H, aromatic ring); 10,48 ppm (s, 2H, –C*H*O).

2.1.3. 2,5-dimethoxyterephthalaldehyde bis(thiophene-2-carbonyl hydrazone)

A 1,0 mmol (0,142 g) 2-thiophenecarboxylic acid hydrazide methanolic solution was added, under constant stirring, to another solution containing 0.5 mmol (0.097 g) of **II** in 10 mL of methanol (**Scheme 1**, bottom). The mixture was refluxed for 2 hours and a yellow solid was formed during this time. The precipitated was filtered off and washed with cold methanol. The resulting yellow solution was maintained at room temperature and, after 7 days, pale orange crystals suitable for X-ray diffraction were separated by filtration. Yield: 0.17 g (76%), m.p. 357-358 ºC. Elemental analysis - Percentages found: C,54.3%; H, 4.1%; N, 12.8%; S, 14.2%. Calcd. for $C_{20}H_{18}O_4N_4S_2$: C, 54.3%; H, 4.1%; N, 12.7%; S, 14.5%. The infrared spectrum of this compound, as well as the 1D and 2D NMR assignments, will be discussed in the Results and Discussion section.

2.2. Instruments and methodology

The determination of carbon, hydrogen, nitrogen and sulfur were performed on a Thermo Electron Corporation CHNS analyzer, model Flash EA 1112. Melting point was determined with a MS TECNOPON Additional equipment LTDA, PMF-11 model, and series 8276.

2.2.1. X-ray crystallography

Single crystal X-ray diffraction (XRD) data for the di-hydrazone were collected on a Bruker D8 Venture diffractometer at room temperature, using Incoatec IμS microfocus X-ray source, MoKα radiation (λ=0.71069 Å). The crystal was mounted on a Kappa Goniometer, and reflections collected using a PHOTON 100 detector. Data collection and cell refinement were performed with Bruker Instrument Service APEX2 v4.2.2 [34]. Data integration was carried out using SAINT [35]. Empirical multiscan absorption correction employing equivalent reflections was achieved with the SADABS program [36]. The structure solutions and full-matrix least-squares refinements based on F^2 were performed with the SHELXS and SHELXL program packages [37]. Anisotropic parameters were refined to all non-hydrogen atoms. Positions concerning the hydrogen atoms were constrained to neutral diffraction distances values [38].

2.2.2. Spectroscopic analyses (FT-IR, Raman, UV-Vis and NMR)

Infrared spectra were recorded on a Perkin-Elmer FT-IR 2000 apparatus. Samples were measured from 4000 to 450 cm^{-1} as KBr pellets. Raman spectra of the solid sample of the di-hydrazone were performed on a Perkin-Elmer Raman Station 400, using the 785 nm line for excitation. Electronic spectra were obtained on a Varian spectrophotometer, model Cary 50 Scan. These analyses were carried on in DMSO solution (10^{-4} mol L^{-1}) at room temperature, by using a 1.0 cm quartz cells. ^{1}H NMR spectrum and the ^{1}H-^{1}H COSY and ^{1}H-^{1}H ROESY (rotating-frame nuclear Overhauser effect spectroscopy, with a mixing time of 200 ms) contour plots of the di-hydrazone were obtained at room temperature in a Bruker Avance III HD-400 spectrometer (9.4 T, 400 MHz for the ^{1}H nuclei) using a 5 mm probe and d_6-DMSO as solvent. Calibration of the spectrum was made with the solvent residual peaks as references (2.50 ppm) [39].

2.2.3. Thermogravimetry

Thermogravimetric analysis of the target compound was performed in a Perkin-Elmer analyzer; model Pyris 1 TGA, under an atmosphere of flowing nitrogen. Temperature was varied from 20 to 900 ºC at a heating rate of 10 ºC min^{-1}.

2.3. *In silico* pharmacological evaluation

Theoretical pharmacological analyses include, as a key process, the investigation of a compound's absorption by the organism. For the target di-hydrazone, this was performed by calculating certain parameters by a 1D-QSAR methodology and then applying the Lipinski rule of five [40]. The calculations involving log *P*, drug score and theoretical solubility were conducted using the Osiris® Property Explorer software. The Wavefunction Spartan 10 v. 1.1.0 package was used for the calculation of the surface electrostatic potential, and structural and QSAR analyses.

3. Results and discussion

3.1. X-ray crystal analysis

Table 1 presents the crystallographic data for 2,5-dimethoxyterephthalaldehyde bis(thiophene-2-carbonyl hydrazone). The crystalline structure belongs to the triclinic system, space group P -1 and *Z*=2. This hydrazonic compound crystallizes in two different conformations, namely, **(a)** and **(b)**,

whose ORTEP representations are displayed in **Figure 1**. The asymmetric unit corresponds to two half-molecules, each of them related to one of the conformers (depicted in yellow in the figure). The symmetrical nature of the molecule is revealed in the crystal structure, as the conformations are located around an inversion center of the space group. **Table 2** shows the bond distances and **Table 3**, some selected angles for both conformers. Simple bonds, such as C5–N1 and C4–C5, allow for free rotation, providing the cited individual conformations. Conformer **(a)** is more linear, while **(b)** is bent around both C5–N1 and $C5^2$–$N1^2$ linkages. This makes **(b)** much more compact, displaying a S1B···$S1B^2$ distance equal to 10.709 Å. In **(a)**, the distance between S1A and $S1A^1$ is 17.585 Å. The carbonyl-tiophene rotation reveals another important difference: **(a)** adopts a *syn* configuration, while the conformation is *anti* in conformer **(b).** This can clearly be observed in the torsion angles presented in **Table 4**. Noteworthy, conformer **(b)** shows an interesting S1···N2 interaction. The key evidence for this is the atoms distance, equal to 2.883(2) Å, which is smaller than the van der Waals radii of both atoms involved (3.35 Å). In order to validate this possibility, we conducted a search in the database center, using IsoStar [41] and defining a S-tiophene interaction with an aromatic sp^2 nitrogen atom. The results pointed out that, from 1,219 interactions, just 418 (34%) display a S···N distance lower than the van der Waals radii. This can be considered as an indicative of nonbonding S···N interaction in the synthesized di-hydrazone.

Despite the differences discussed above, there are some common aspects to both conformations: C5–O1 and C5–N1 distances suggest that conformers **(a)** and **(b)** are in the *keto* (amide) form. Moreover, all the hydrazonic N2=C6 bonds correspond to the (*E*) isomer. Both conformations are almost planar, since the angle deviation of the thiophene heterocycles in relation to the aromatic central ring is equal to 9.3(3) and 26.3(3)º for **(a)** and **(b)**, respectively.

An intricate network of conventional and unconventional moderate to weak intermolecular H-bonds (**Table 5**) gives rise to a 3D supramolecular structure. The Hirshfeld surface analysis (**Figure 2**) indicates that the foremost contributions to the lattice stabilization come from H...H, O…H and C...H interactions. Conformers **(a)** and **(b)** are perpendicularly oriented in the structure (**Figure 3**) and there are π-π stacking interactions involving the central and the thiophene rings of **(a)**, with a centroid-centroid distance equal to 3.798(1) Å.

Table 1. Crystallographic data for the target di-hydrazone

Formula	$C_{20}H_{18}O_4N_4S_2$
Weight (g mol^{-1})	442.5
Crystal System	Triclinic
Space Group	P -1
a (Å)	8.8631(6)
b (Å)	9.6956(7)
c (Å)	12.6422(8)
α (°)	79.850(2)
β (°)	80.813(2)
γ (°)	71.011(2)
V ($Å^3$)	1005.06(12)
Z	2
$d_{calc.}$ (g cm^{-3})	1.462
μ (MoK_α = 0.71073) (mm^{-1})	0.301
I_{obs} / $I_{obs}>2\sigma(I_{obs})$	3950 / 3104
Nº. of refined parameters	271
R (F_o^2 / $F_o^2>2\sigma F_o^2$)	0.0708 / 0.0531
wR	0.1442
S	1.056
RMS_{peak} (e^- $Å^{-3}$)	0.072

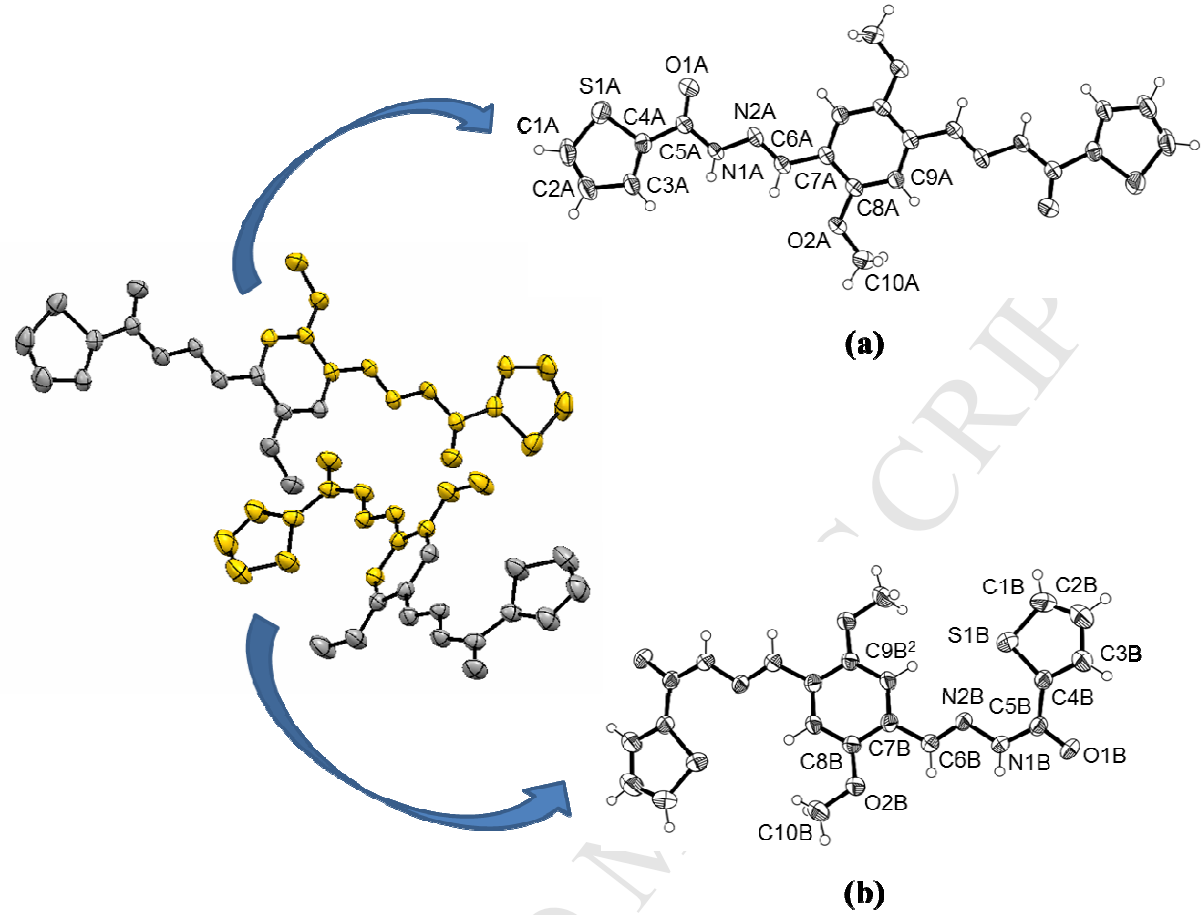

Figure 1. ORTEP representations of conformers **(a)** and **(b)** in the structure of 2,5-dimethoxyterephthalaldehyde bis(thiophene-2-carbonyl hydrazone). Thermal ellipsoids are shown at 50% probability level. Asymmetric units, with the hydrogen atoms omitted for the sake of clarity, are highlighted in yellow (left side).

Table 2. Bond distances (Å) for conformations **(a)** and **(b)** of the target di-hydrazone

Conformer (a)		**Conformer (b)**	
Bond	**Distance**	**Bond**	**Distance**
S1A–C1A	1.689(4)	S1B–C1B	1.700(4)
S1A–C4A	1.707(3)	S1B–C4B	1.712(3)
C1A–C2A	1.338(5)	C1B–C2B	1.347(5)
C2A–C3A	1.424(4)	C2B–C3B	1.386(5)
C3A–C4A	1.383(4)	C3B–C4B	1.392(4)
C4A–C5A	1.477(3)	C4B–C5B	1.474(4)
C5A–O1A	1.221(3)	C5B–O1B	1.232(3)
C5A–N1A	1.354(3)	C5B–N1B	1.346(3)
N1A–N2A	1.380(3)	N1B–N2B	1.374(3)
N2A–C6A	1.271(3)	N2B–C6B	1.275(3)
C6A–C7A	1.463(3)	C6B–C7B	1.467(4)
C7A–C8A	1.402(3)	C7B–C8B	1.402(4)
C7A–C9A[1]	1.395(3)	C7B–C9B[2]	1.391(4)
C8A–C9A	1.378(3)	C8B–C9B	1.382(4)
C8A–O2A	1.371(3)	C8B–O2B	1.365(3)
C9A–C7A[1]	1.395(3)	C9B[2]–C8B[2]	1.382(4)
O2A–C10A	1.406(4)	O2B–C10B	1.419(4)

Symmetry codes: [1] $1 - x, 1 - y, -z$; [2] $1 - x, -y, 1 - z$

Table 3. Bond angles (º) for conformations **(a)** and **(b)** of the target di-hydrazone

Conformer (a)		**Conformer (b)**	
Atoms	**Angle**	**Atoms**	**Angle**
C1A–S1A–C4A	91.81(15)	C1B–S1B–C4B	91.67(16)
C2A–C1A–S1A	112.7(2)	C2B–C1B–S1B	112.6(3)
C1A–C2A–C3A	113.1(3)	C1B–C2B–C3B	112.6(3)
C2A–C3A–C4A	110.7(3)	C2B–C3B–C4B	113.0(3)
C3A–C4A–S1A	111.61(19)	C3B–C4B–S1B	110.1(2)
C3A–C4A–C5A	130.2(2)	C3B–C4B–C5B	121.1(3)
C5A–C4A–S1A	118.1(2)	C5B–C4B–S1B	128.8(2)
O1A–C5A–C4A	122.2(2)	O1B–C5B–C4B	119.5(2)
O1A–C5A–N1A	123.3(2)	O1B–C5B–N1B	118.8(2)
N1A–C5A–C4A	114.5(2)	N1B–C5B–C4B	121.7(2)
C5A–N1A–N2A	119.6(2)	C5B–N1B–N2B	122.6(2)
C6A–N2A–N1A	114.4(2)	C6B–N2B–N1B	115.4(2)
N2A–C6A–C7A	121.9(2)	N2B–C6B–C7B	120.2(2)
C8A–C7A–C6A	118.7(2)	C8B–C7B–C6B	120.4(2)
C9A[1]–C7A–C6A	122.2(2)	C9B[2]–C7B–C6B	120.6(2)
C9A[1]–C7A–C8A	119.1(2)	C9B[2]–C7B–C8B	119.0(2)
C9A–C8A–C7A	120.5(2)	C9B–C8B–C7B	119.8(2)
O2A–C8A–C7A	115.1(2)	O2B–C8B–C7B	116.5(2)
O2A–C8A–C9A	124.4(2)	O2B–C8B–C9B	123.7(2)
C8A–C9A–C7A[1]	120.4(2)	C8B[2]–C9B[2]–C7B	121.2(2)
C8A–O2A–C10A	118.4(2)	C8B–O2B–C10B	117.3(2)

Symmetry codes: [1] 1 – *x*, 1 – *y*, –*z*; [2] 1 – *x*, –*y*, 1 – *z*

Table 4. Selected torsion angles (º) for conformations **(a)** and **(b)** of the target di-hydrazone

Atoms	Conformer (a)	Conformer (b)
C4–C5–N1–N2	–174.0(2)	–7.1(4)
O1–C5–N1–N2	5.3(4)	172.6(2)
S1–C4–C5–O1	0.0(4)	172.8(2)
S1–C4–C5–N1	179.3(2)	–7.4(4)
C3–C4–C5–O1	–177.4(3)	–5.9(4)
C3–C4–C5–N1	1.9(4)	173.8(3)
C5–N1–N2–C6	178.4(2)	–167.9(2)
N1–N2–C6–C7	–179.7(2)	178.5(2)

Table 5. Intermolecular H-bonding parameters for conformations **(a)** and **(b)** of the target di-hydrazone

Donor–H	Acceptor	*d*(D–H)/Å	*d*(H···A)/Å	*d*(D–A)/Å	<DHA/º
N1B–H	O1A	0.86	2.19	3.017(3)	160.4
N1B–H	N2A	0.86	2.53	3.115(3)	126.4
C6B–H6B	O1A	0.93	2.63	3.381(3)	138.1
N1A–H	O1B*	0.86	2.17	3.003(3)	162.1
C3A–H3A	O1B*	0.93	2.59	3.463(4)	157.4
C6A–H6A	O1B*	0.93	2.44	3.281(3)	149.7
C10A–H10A''	S1A*	0.96	2.91	3.691(4)	139.0
C10A–H10A'''	S1B**	0.96	2.98	3.818(4)	146.6
C3B–H3B	S1A***	0.93	2.87	3.741(3)	155.6

Symmetry codes: * $-x, 1-y, -z$; ** $1-x, 1-y, -z$; *** $x, 1+y, z$

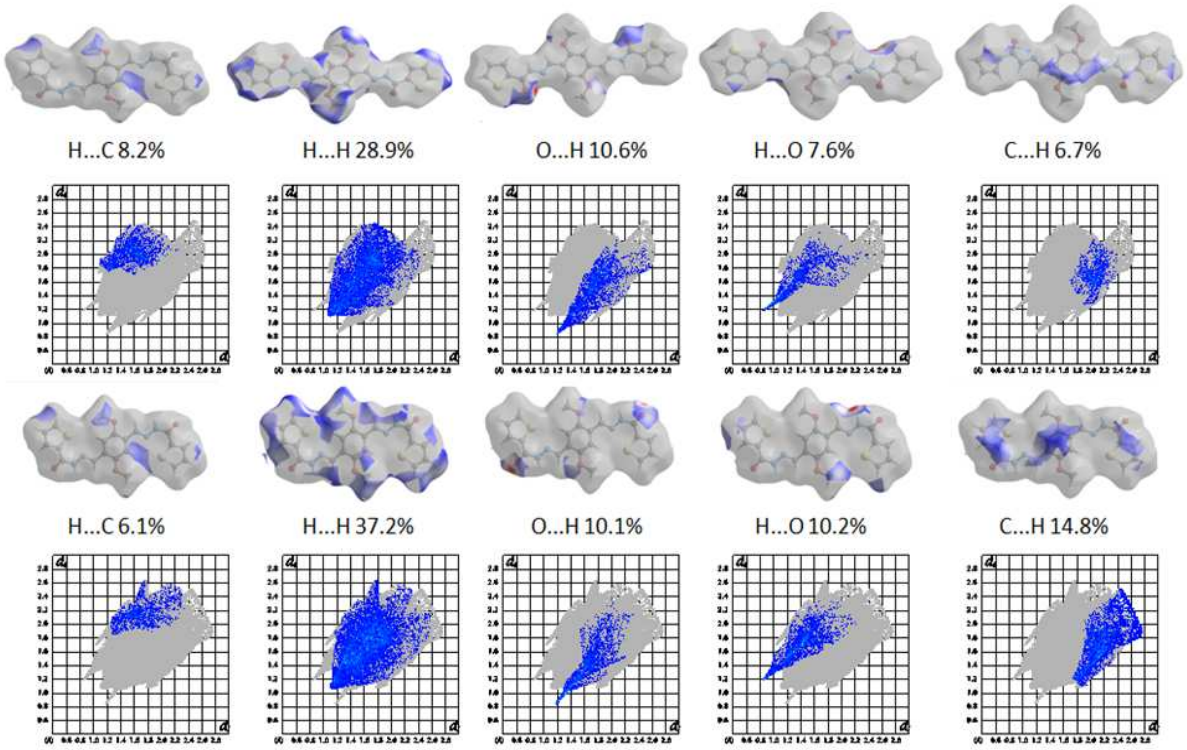

Figure 2. Hirshfeld surfaces, with the corresponding fingerprint plots broken down into contributions (%) from specific pairs of atom-types, for conformations **(a)**, top, and **(b)**, bottom, of the target di-hydrazone.

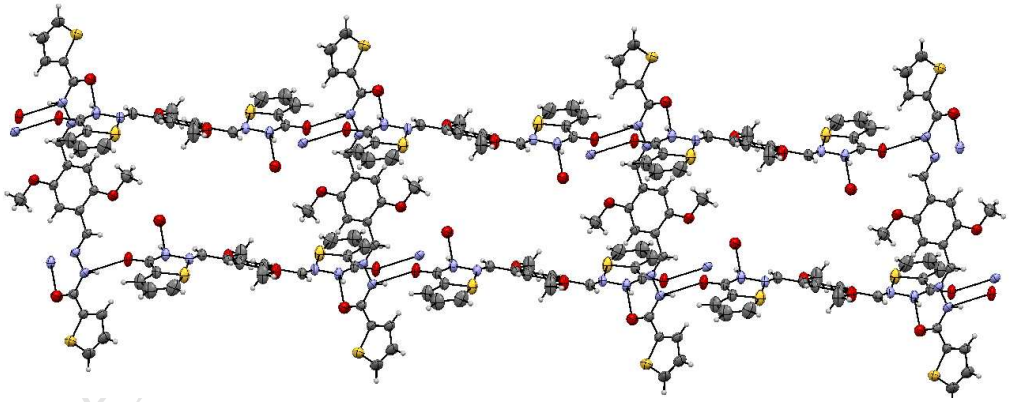

Figure 3. Representation of the perpendicular disposition that conformations **(a)** and **(b)** adopt in the lattice.

3.2. Vibrational spectroscopy

Figure 4 displays the infrared (top) and Raman (bottom) spectra of the di-hydrazone, while **Table 6** lists some selected (stretching) vibrational absorptions, along with their respective assignments.

A comparative analysis of the infrared spectra of 2,5-dimethoxyterephthalaldehyde bis(thiophene-2-carbonyl hydrazone) and that of its di-aldehyde precursor **II** (**Figure S1**, Supplementary material) provides important information concerning the obtention of the target compound. For example, the frequencies related to the aldehydes' ν(C–H) and ν(C=O) modes, appearing at, respectively, 2870 and 1679 cm^{-1} in the spectrum of **II** are not observed in the FT-IR spectrum of the di-hydrazone indicating the absence of such groups in the final product. Instead, a rather broad and intense IR band at 1640 cm^{-1} (observed as a weak peak in the Raman spectrum) associated to the ν(C=O) and ν(C=N) modes of carbonyl hydrazones, which are in this case overlapped, prove the attachment of the 2-thiophenecarbonyl-derived arms to the precursor center **II** through a condensation reaction. In fact, the C=N stretching modes of azomethine groups show absorptions close to that of carbonyl stretchings [42]. This fact can sometimes difficult an accurate assignment. Also, the IR spectrum of the target compound shows characteristic hydrazone bands at 3162 and 1135 (1124 cm^{-1} in Raman) cm^{-1}, which can be ascribed, correspondingly, to the ν(N–H) and ν(N–N) frequencies. These values are in agreement with those observed for similar compounds [43, 44].

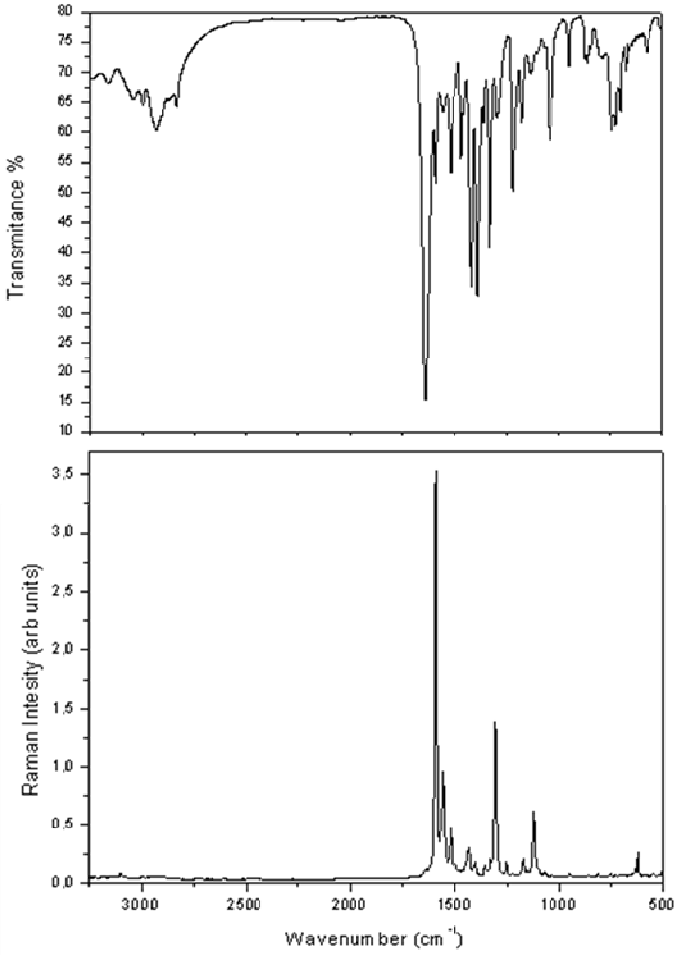

Figure 4. Infrared (top) and Raman (bottom) spectra of the target di-hydrazone in the range 3250-500 cm^{-1}.

Table 6. Selected infrared and Raman absorptions, with their respective assignments

FT-IR (cm^{-1})	Raman (cm^{-1})	Assignment
3162	-	ν(N–H)
3078, 3045	-	$\nu(C–H)_{arom.}$
2999	-	$\nu_{as}(C–H)_{methyl}$
2953, 2937, 2903	-	$\nu_{s}(C–H)_{methyl}$
1640	1640	ν(C=O) + $\nu(C=N)_{azomethine}$
1591, 1554, 1518	1594, 1560, 1520	$\nu(C=C)_{thiophene}$
1465, 1454, 1416	- , 1448 , -	$\nu(C=C)_{central\ ring}$
1219	1226	$\nu_{ass}(C–O–C)$
1135	1124	ν(N–N)
1043	1037	$\nu_{s}(C–O–C)$
858	860	$\nu_{ass}(C–S–C)_{thiophene}$
845	-	$\nu_{s}(C–S–C)_{thiophene}$
757	756	ν(C–S)

The carbon-carbon stretching modes of the thiophene rings and the benzene central ring are very well separated in the vibrational spectra of the di-hydrazone, with those related to the heterocycles being observed at higher wavenumbers. The parallel analysis of the IR spectra of the precursors **II** and 2-thiophenecarboxylic acid hydrazide (**Figure S2**, Supplementary material) assisted us in the assignment of these bands. Whereas the thiophene rings originate absorptions at 1591, 1554 and 1518 cm^{-1} (1594, 1560 and 1520 cm^{-1} in the Raman spectrum), the central ring is associated to a series of bands at 1465, 1454 and 1416 cm^{-1}. Hydrogen-containing aromatic rings usually exhibit multiple weak bands in the region 3100-3000 cm^{-1} due to C–H stretching vibrations. In the present case, these vibrations are registered at 3078 and 3045 cm^{-1} in the IR spectrum [45].

The presence of the thiophene ring was confirmed by its characteristic stretching bands involving the sulfur atom. The IR absorptions at 858 [ν_{ass}(C–S–C)], 845 [ν_{s}(C–S–C)] and 757 cm^{-1} [ν(C–S)] were, in this context, fundamental in order to identify the heterocycle in the target compound [46].

On the other hand, the asymmetric and symmetric stretching modes of the methoxyl substituents in the central ring are observed, respectively, at 1219 and 1043 cm^{-1} in FT-IR. These modes appear, correspondingly, at 1226 and 1037 cm^{-1} in the Raman spectrum. The C–H stretching vibrations of the methoxyl groups occur at 2999, 2953, 2937, and 2903 cm^{-1} [47].

3.3. Electronic spectroscopy

The UV-Vis spectrum of 2,5-dimethoxyterephthalaldehyde bis(thiophene-2-carbonyl hydrazone) is shown in **Figure 5**, along with those of its synthetic precursors **II** and 2-thiophenecarboxylic acid hydrazide. In a similar way to that observed for the previously published isonicotinoyl hydrazone of *o*-vanillin [17], there are two well-defined groups of bands, being the more energetic absorptions related to $\pi \rightarrow \pi^*$ transitions. These bands, detected at 329 (ε = 5600 L mol^{-1} cm^{-1}) and 347 nm (5300 L mol^{-1} cm^{-1}), are red-shifted when compared to those of the compound in the cited reference due to the more delocalized nature of a di-hydrazone.

On the other hand, $n \rightarrow \pi^*$ transitions (responsible for the color of the di-hydrazone) appear as an intense band at 395 nm (ε = 7500 L mol^{-1} cm^{-1}) with a shoulder at 414 nm (6400 L mol^{-1} cm^{-1}). The band is closely related to that observed in the spectrum of precursor **II** (395 nm, 2100 L mol^{-1} cm^{-1}).

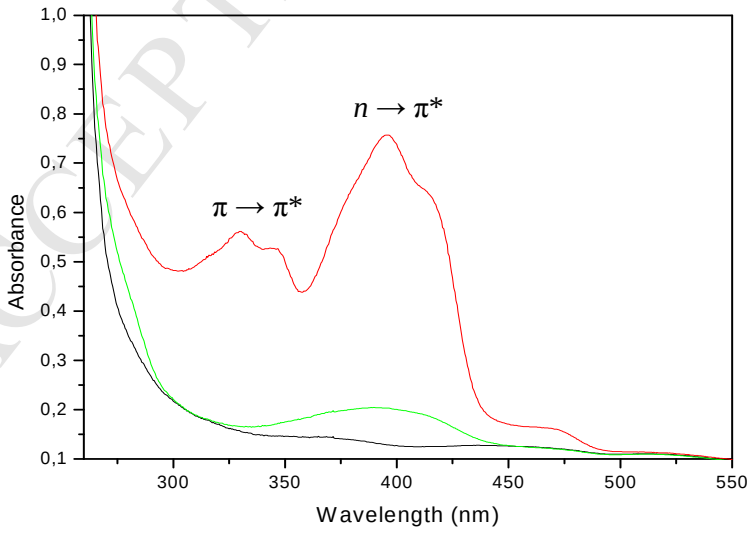

Figure 5. Electronic absorption spectra of the precursors **II** (green line) and 2-thiophenecarboxylic acid hydrazide (black line), as well as that of the resulting di-hydrazone (red line) in the range 280-550 nm. [ ] = 10^{-4} mol L^{-1}.

3.4. NMR spectral studies

For a better allocation of the di-hydrazone ^{1}H NMR spectrum, a 2D COSY contour plot (**Figure 6**) was used in order to correlate vicinal hydrogens. All the hydrogens present in the molecule were found and **Table 7** shows the proposed assignments, along with other useful information.

Despite the symmetric nature of the compound, two well-defined sets of associated signals are observed in the 1D spectrum of the di-hydrazone, indicating that the symmetry of the molecule is broken by some kind of intra- or intermolecular interactions. This effect probably involves rotation around single bonds, which, as seen from the crystal structure of the compound, lead to conformers with small energy differences between them. The most affected, i.e. more separated, signals are those related to the azomethine (H6/H6*) hydrogens, followed by the central ring (H9/H9*), some of the thiophene rings (H1/H1* and H3/H3*) and, finally, the –NH hydrogens. On the other hand, the methoxyl (H10/H10*) and, mainly, the thiophene-related H2/H2* hydrogen atoms are virtually equivalent. With the help of a ^{1}H-^{1}H ROESY contour plot, we were able to observe through-space correlations between H6/H6* and –NH hydrogens, as well as between –NH and H3/H3*. The latter implies that, in solution, the hydrazonic lateral chains of the molecule are in a conformation similar to the one in conformer **(a)**, i.e. a *syn* configuration. Another hypothesis is that free-rotation around single bonds exceed the NMR chemical shift timescale. However, the reason behind the non-equivalency of some hydrogens in this symmetric di-hydrazone remains unclear.

Table 7. ^{1}H NMR chemical shifts, in ppm, for the target di-hydrazone (d_6-DMSO) at room temperature. See Figure 6, inset, for a complete atom labeling scheme, which is in agreement with the crystallographic number system

Atom	δ
N1H / N1H*	11.99 (s, 1H) / 11.94 (s, 1H)
H6 / H6*	8.79 (s, 1H) / 8.43 (s, 1H)
H3 / H3*	8.06 (d, 1H, $^{3}J_{HH}$ ~ 4.0) / 7.95 (d, 1H, $^{3}J_{HH}$ ~ 4.0)
H1 / H1*	7.98 (d, 1H, $^{3}J_{HH}$ ~ 4.0) / 7.88 (d, 1H, $^{3}J_{HH}$ ~ 4.0)
H9 / H9*	7.69 (s, 1H) / 7.52 (s, 1H)

H2 / H2*	7.23 (t, 2H, $^{3}J_{HH}$ ~ 4.0)
H10 / H10*	3.93 (s, 3H) / 3.89 (s, 3H)

The signal multiplicities, as well as their respective integration and coupling constants (*J*, Hz) are in parentheses

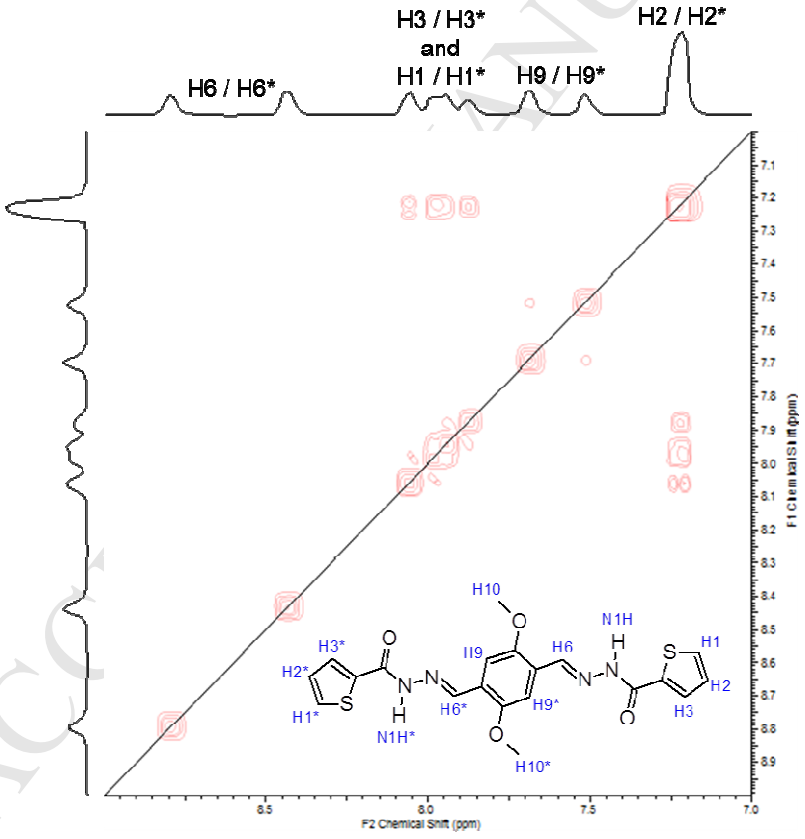

Figure 6. Section of the ^{1}H-^{1}H COSY contour plot of the target di-hydrazone, displaying the aromatic region.

3.5. Thermogravimetric analysis

From the thermal decomposition curve of the compound, we observed the absence of crystallization solvent in the structure, because there is no significant mass loss below 300 ºC. This information is

confirmed by the XRD analysis, as discussed above. Between 350 and 390 ºC, with a maximum decomposition rate at 372 ºC, an important and well-defined weight loss, corresponding to 72.3% of the initial mass, takes place. As the observed melting point for the compound is around 357-358 ºC, this phase transition is certainly associated to chemical transformations of the di-hydrazone.

3.6. Computational pharmacological evaluation

Table 8 presents some important theoretical parameters calculated for the di-hydrazone, along with some reference values. Most parameters are within the desired ranges for good oral bioavailability, with the polar surface area (PSA) being a little higher than the upper limit. On the other hand, the calculated aqueous solubility of the compound is too low, which can be overcome through the use of an adequate delivery system or by a salt (for example, hydrochloride) formation strategy. Based on these parameters, the drug score of the compound, an estimate of the probability the substance has to become an actual drug, can be calculated. This di-hydrazone displays a drug score of 45%.

Table 8. Performance of the target di-hydrazone concerning some molecular properties relevant for a drug's pharmacokinetics in the human body, along with reference values

	di-hydrazone	**Reference values**
MW (g mol^{-1})	442	≤ 500
HBD	2	≤ 5
HBA	10	≤ 10
PSA ($Å^2$)	157.8	≤ 140
Calcd. log *P*	4.34	≤ 5
Calcd. log *S*	–5.88	≥ –4
Rotatable bonds	10	≤ 10
Drug score	0.45	-

MW – molecular weight; HBD – H-bond donors; HBA – H-bond acceptors; PSA – polar surface area

Altogether, the *in silico* results indicate that the synthesized compound possesses some molecular properties important for a drug's pharmacokinetics in the human body. However, the Lipinski rule does not predict if a specific compound is pharmacologically active.

4. Conclusions

A novel di-hydrazone derived from 2-thiophenecarboxylic acid hydrazide was synthesized in good yields through a protocol involving a condensation reaction with a terephthalaldehyde derivative. The compound crystallizes in two different conformations, one more linear and the other, bent. Interesting intramolecular S···N interactions seem to be involved in the stabilization of the latter. All the hydrazonic bonds correspond, however, to (*E*) isomers. There is no crystallization solvent. Distinctive IR and Raman bands denote hydrazone formation, as well as the presence of the thiophene rings. This compound melts at 357-358 ºC in a process that comprises an important loss of weight (thermal decomposition). The solution ^{1}H NMR spectrum of the substance exhibits two well-defined sets of signals, which is, *a priori*, unexpected for such a symmetric molecule. The ^{1}H-^{1}H ROESY experiment suggests a *syn* configuration for the hydrazonic lateral chains. Finally, this di-hydrazone performs quite well concerning the Lipinski rule of five, presenting a drug score of 45%. The compound is being screened towards a series of biological activities and the results will be the subject of future reports.

Supplementary information

IR spectra of the synthetic precursors **II** and 2-thiophenecarboxylic acid hydrazide in the range 4000-450 cm^{-1}. CCDC 1413069 contains the supplementary crystallographic data for this paper. These data can be obtained free of charge via http://www.ccdc.cam.ac.uk/conts/retrieving.html (or from the Cambridge Crystallographic Data Centre, 12, Union Road, Cambridge CB2 1EZ, UK; fax: +44 1223 336033).

Acknowledgments

Nicolás A. Rey wishes to thank FAPERJ (Fundação Carlos Chagas Filho de Amparo à Pesquisa do Estado do Rio de Janeiro, Brazil) and CNPq (Conselho Nacional de Desenvolvimento Científico e Tecnológico, Brazil) for the research fellowships awarded. The authors are indebted to Rosana Garrido Gomes for her invaluable help in the NMR analyses, performed in the Central Analytical Facility of the Department of Chemistry (PUC-Rio).

References

[1] I. Kostova, L. Saso, Advances in Research of Schiff-Base Metal Complexes as Potent Antioxidants, Current Medicinal Chemistry, 20 (2013) 4609-4632.
[2] M. Asif, A. Husain, Analgesic, Anti-Inflammatory, and Antiplatelet Profile of Hydrazones Containing Synthetic Molecules, Journal of Applied Chemistry, 2013 (2013) 1-7.

[3] S. Rollas, S.G. Kucukguzel, Biological activities of hydrazone derivatives, Molecules, 12 (2007) 1910-1939.
[4] P.C. Lima, L.M. Lima, K.C.M. da Silva, P.H.O. Leda, A.L.P. de Miranda, C.A.M. Fraga, E.J. Barreiro, Synthesis and analgesic activity of novel N-acylarylhydrazones and isosters, derived from natural safrole, European Journal of Medicinal Chemistry, 35 (2000) 187-203.
[5] S. Kumar, S. Bawa, S. Drabu, R. Kumar, L. Machawal, Synthesis and in Vivo Anticonvulsant Evaluation of 2-Chloroquinolinyl Hydrazone Derivatives, Acta Poloniae Pharmaceutica, 67 (2010) 567-573.
[6] F.R. Pavan, P.I.D. Maia, S.R.A. Leite, V.M. Deflon, A.A. Batista, D.N. Sato, S.G. Franzblau, C.Q.F. Leite, Thiosemicarbazones, semicarbazones, dithiocarbazates and hydrazide/hydrazones: Anti-Mycobacterium tuberculosis activity and cytotoxicity, European Journal of Medicinal Chemistry, 45 (2010) 1898-1905.
[7] A. Ozdemir, Z.A. Kaplanckikli, G. Turan-Zitouni, G. Revial, Synthesis of some novel hydrazone derivatives and evaluation of their antituberculosis activity, Marmara Pharmaceutical Journal, 14 (2010) 79-83.
[8] S.A.M. El-Hawash, A.E.A. Wahab, M.A. El-Demellawy, Cyanoacetic acid hydrazones of 3-(and 4-)acetylpyridine and some derived ring systems as potential antitumor and anti-HCV agents, Archiv Der Pharmazie, 339 (2006) 14-23.
[9] P. Vicini, M. Incerti, I.A. Doytchinova, P. La Colla, B. Busonera, R. Loddo, Synthesis and antiproliferative activity of benzo[d]isothiazole hydrazones, European Journal of Medicinal Chemistry, 41 (2006) 624-632.
[10] L. Savini, L. Chiasserini, V. Travagli, C. Pellerano, E. Novellino, S. Cosentino, M.B. Pisano, New alpha-(N)-heterocyclichydrazones: evaluation of anticancer, anti-HIV and antimicrobial activity, European Journal of Medicinal Chemistry, 39 (2004) 113-122.
[11] P. Vicini, M. Incerti, P. La Colla, R. Loddo, Anti-HIV evaluation of benzo[d]isothiazole hydrazones, European Journal of Medicinal Chemistry, 44 (2009) 1801-1807.
[12] P. Melnyk, V. Leroux, C. Sergheraert, P. Grellier, Design, synthesis and in vitro antimalarial activity of an acylhydrazone library, Bioorganic & Medicinal Chemistry Letters, 16 (2006) 31-35.
[13] R.M. Mohareb, K.A. El-Sharkawy, M.M. Hussein, H.M. El-Sehrawi, Synthesis of hydrazide-hydrazone derivatives and their evaluation of antidepressant, sedative and analgesic agents, J. Pharm. Sci. & Res., 2 (2010) 185-196.
[14] A.G. Silva, G. Zapata-Sudo, A.E. Kummerle, C.A.M. Fraga, E.J. Barreiro, R.T. Sudo, Synthesis and vasodilatory activity of new N-acylhydrazone derivatives, designed as LASSBio-294 analogues, Bioorganic & Medicinal Chemistry, 13 (2005) 3431-3437.
[15] L.M.F. Gomes, R.P. Vieira, M.R. Jones, M.C.P. Wang, C. Dyrager, E.M. Souza-Fagundes, J.G. Da Silva, T. Storr, H. Beraldo, 8-Hydroxyquinoline Schiff-base compounds as antioxidants and modulators of copper-mediated A beta peptide aggregation, Journal of Inorganic Biochemistry, 139 (2014) 106-116.
[16] R.A. Hauser-Davis, L.V. de Freitas, D.S. Cukierman, W.S. Cruz, M.C. Miotto, J. Landeira-Fernandez, A.A. Valiente-Gabioud, C.O. Fernandez, N.A. Rey, Disruption of zinc and copper interactions with A beta(1-40) by a non-toxic, isoniazid-derived, hydrazone: a novel biometal homeostasis restoring agent in Alzheimer's disease therapy?, Metallomics, 7 (2015) 743-747.
[17] A.C. Gonzalez-Baro, R. Pis-Diez, B.S. Parajon-Costa, N.A. Rey, Spectroscopic and theoretical study of the o-vanillin hydrazone of the mycobactericidal drug isoniazid, Journal of Molecular Structure, 1007 (2012) 95-101.
[18] L.V. de Freitas, C.C.P. da Silva, J. Ellena, L.A.S. Costa, N.A. Rey, Structural and vibrational study of 8-hydroxyquinoline-2-carboxaldehyde isonicotinoyl hydrazone - A potential metal-protein attenuating compound (MPAC) for the treatment of Alzheimer's disease, Spectrochimica Acta Part a-Molecular and Biomolecular Spectroscopy, 116 (2013) 41-48.

[19] R. Mishra, K.K. Jha, S. Kumar, I. Tomer, Synthesis, properties and biological activity of thiophene: A review, Der Pharma Chemica, 3 (2011) 38-54.
[20] A. Chaudhary, K.K. Jha, S. Kumar, Biological diversity of Thiophene: A review, Journal of Advanced Scientific Research, 3 (2012) 3-10.
[21] S. Bondock, W. Fadaly, M.A. Metwally, Synthesis and antimicrobial activity of some new thiazole, thiophene and pyrazole derivatives containing benzothiazole moiety, European Journal of Medicinal Chemistry, 45 (2010) 3692-3701.
[22] R. Mishra, I. Tomer, S. Kumar, Synthesis and antimicrobial evaluation of novel thiophene derivatives, Der Pharmacia Sinica, 3 (2012) 332-336.
[23] R.A. Forsch, J.E. Wright, A. Rosowsky, Synthesis and in vitro antitumor activity of thiophene analogues of 5-chloro-5,8-dideazafolic acid and 2-methyl-2-desamino-5-chloro-5,8-dideazafolic acid, Bioorganic & Medicinal Chemistry, 10 (2002) 2067-2076.
[24] K.I. Molvi, K.K. Vasu, S.G. Yerande, V. Sudarsanam, N. Haque, Syntheses of new tetrasubstituted thiophenes as novel anti-inflammatory agents, European Journal of Medicinal Chemistry, 42 (2007) 1049-1058.
[25] K.K. Jha, S. Kumar, I. Tomer, R. Mishra, Thiophene: The molecule of diverse medicinal importance, Journal of Pharmacy Research, 5 (2012) 560-566.
[26] J.L. Duffy, B.A. Kirk, Z. Konteatis, E.L. Campbell, R. Liang, E.J. Brady, M.R. Candelore, V.D.H. Ding, G.Q. Jiang, F. Liu, S.A. Qureshi, R. Saperstein, D. Szalkowski, S. Tong, L.M. Tota, D. Xie, X.D. Yang, P. Zafian, S. Zheng, K.T. Chapman, B.B. Zhang, J.R. Tata, Discovery and investigation of a novel class of thiophene-derived antagonists of the human glucagon receptor, Bioorganic & Medicinal Chemistry Letters, 15 (2005) 1401-1405.
[27] W.W. Wardakhan, O.M.E. Abdel-Salam, G.A. Elmegeed, Screening for antidepressant, sedative and analgesic activities of novel fused thiophene derivatives, Acta Pharmaceutica, 58 (2008) 1-14.
[28] O.I. Abd El-Salam, A.M. Shalaby, A.A. El-Sawy, S. Elshihaby, M. Abdulla, Synthesis of Some N-[(4-Substituted-1-Piperazinyl)-Oxo(Alkyl and Ethylcarbamoyl)]-3-(2-Thiophenyl)Acrylamides as Non-Steroidal Anti-Allergic and Anti-Inflammatory Agents, Open Journal of Synthesis Theory and Applications, 2 (2013) 63-72.
[29] Y. Tian, X. Wei, H. Xu, Photoactivated Insecticidal Thiophene Derivatives from *Xanthopappus subacaulis*, J. Nat. Prod., 69 (2006) 1241-1244.
[30] A.A. Fadda, M.A. Berghot, F.A. Amer, D.S. Badawy, N.M. Bayoumy, Synthesis and Antioxidant and Antitumor Activity of Novel Pyridine, Chromene, Thiophene and Thiazole Derivatives, Archiv Der Pharmazie, 345 (2012) 378-385.
[31] A. Dreiem, F. Fonnum, Thiophene is toxic to cerebellar granule cells in culture after bioactivation by rat liver enzymes, Neurotoxicology, 25 (2004) 959-966.
[32] R. Ando, H. Ono, T. Yagyu, M. Maeda, Spectroscopic characterization of mononuclear, binuclear, and insoluble polynuclear oxovanadium(IV)–Schiff base complexes and their oxidation catalysis, Inorganica Chimica Acta, 357 (2004) 817–823.
[33] K.B. Borisenko, K. Zauer, I. Hargittai, Intramolecular Hydrogen Bonding and Molecular Structure of 2,5-Dihydroxyterephthalaldehyde and 4,6-Dihydroxyisophthalaldehyde: A Gas-Phase Electron Diffraction and ab Initio Molecular Orbital Study, J. Phys. Chem., 100 (1996) 19303-19309.
[34] Bruker, APEX2 User Manual Version 1.22, (2004).
[35] Bruker, SAINT Integration Spftware. v8.34A. Bruker AXS Inc., Madison, Wisconsin, USA. 1999.
[36] G.M. Sheldrick, SADABS, Program for Empirical Absorption Correction of Area Detector Data, University of Göttingen, Germany, 1996.
[37] G.M. Sheldrick, Crystal structure refinement with SHELXL, Acta Crystallogr. C Struct. Chem., 71 (2015) 3-8.

[38] International Tables for Crystallography C, 790-811., (2006).
[39] S. Hingorani, B.V. Agarwala, Structural Elucidation of O-Vanillin Isonicotinoyl Hydrazone and Its Metal-Complexes, Transition Metal Chemistry, 18 (1993) 576-578.
[40] C.A. Lipinski, F. Lombardo, B.W. Dominy, P.J. Feeney, Experimental and computational approaches to estimate solubility and permeability in drug discovery and development settings, Adv. Drug Delivery Rev., 23 (1997) 3–25.
[41] Cambridge Crystallographic Data Centre - IsoStar User Guide and Tutorials 2014.
[42] A.A.R. Despaigne, L.F. Vieira, I.C. Mendes, F.B. da Costa, N.L. Speziali, H. Beraldo, Organotin(IV) Complexes with 2-Acetylpyridine Benzoyl Hydrazones: Antimicrobial Activity, Journal of the Brazilian Chemical Society, 21 (2010) 1247-1257.
[43] S. Devi, A.M. Singh, Synthesis and Characterisation of Cobalt(II) Complexes with Benzil Isonicotinoyl Hydrazone O. , J. Chem. Pharm. Res., 3 (2011) 1055-1060.
[44] E.A. Mohamed, K. Kennouche Youness, M. Hamidi M. El, Synthesis and characterization of salicylaldazine (H_2L) and its mixed ligand complexes [$ML(H_2O)$], [$M(LH)_2(caf)_n$] ; M= Zn^{2+}, Cd^{2+}, Ni^{2+}, Cu^{2+},Co^{2+}, Mn^{2+}, $Fe2^{+}$; n=1,2 ; Caf= caffeine, Research Journal of Chemical Sciences, 4 (2014) 72-84.
[45] H.W. Thompson, R.B. Temple, The infra-red spectra of furan and thiophen, in: E.M. Frith (Ed.)1944.
[46] M. Arora, J. Saravanan, S. Mohan, S. Bhattacharjee, Synthesis, characterization and antimicrobial activity of some schiff bases of 2-amino-N-(P-acetamidophenyl carboxamido)-4,5,6,7-tetramethylene thiophenes, International Journal of Pharmacy and Pharmaceutical Sciences, 5 (2013).
[47] W.C. Wu, C.C. Chuang, J.L. Lin, Bonding geometry and reactivity of methoxy and ethoxy groups adsorbed on powdered TiO2, Journal of Physical Chemistry B, 104 (2000) 8719-8724.

Highlights

- A novel di-hydrazone containing thiophene heterocyclic rings was synthesized.
- This symmetrical compound crystallizes in two different conformations.
- Its solution ^{1}H NMR spectrum exhibits some unexpected non-symmetric features.
- This di-hydrazone performs quite well concerning the Lipinski rule of five.